Available online at www.sciencedirect.com
ScienceDirect
Nanomedicine: Nanotechnology, Biology, and Medicine 4 (2008) 283–294
nanomedicine
www.nanomedjournal.com

Original Article: Neurology

SOD Activity of carboxyfullerenes predicts their neuroprotective efficacy: a structure-activity study

Sameh Saad Ali, PhD,[a,*] Joshua I. Hardt, BS,[b] Laura L. Dugan, MD[a,c]

[a]*Department of Medicine, University of California, San Diego, California*
[b]*Department of Neurology, Washington University School of Medicine, St. Louis Missouri*
[c]*Departments of Medicine and Neurosciences, University of California, San Diego, California, USA*

Abstract Superoxide radical anion is a biologically important oxidant that has been linked to tissue injury and inflammation in several diseases. Here we carried out a structure-activity study on six different carboxyfullerene superoxide dismutase (SOD) mimetics with distinct electronic and biophysical characteristics. Neurotoxicity via *N*-methyl-D-aspartate receptors, which involves intracellular superoxide, was used as a model to evaluate structure-activity relationships between reactivity toward superoxide and neuronal rescue by these drugs. A significant correlation between neuroprotection by carboxyfullerenes and their k_i toward superoxide radical was observed. Computer-assisted molecular modeling demonstrated that the reactivity toward superoxide is sensitive to changes in dipole moment, which are dictated not only by the number of carboxyl groups but also by their distribution on the fullerene ball. These results indicate that the SOD activity of these cell-permeable compounds predicts neuroprotection, and establishes a structure-activity relationship to aid in future studies on the biology of superoxide across disciplines.

Key words: Superoxide; Neuroprotection; Carboxyfullerenes; SOD mimetics

Superoxide radical is a biologically important reactive oxygen species (ROS) that is proposed to contribute to inflammation, altered cellular metabolism, and tissue injury in diabetes, stroke, cardiovascular disease, and cancer. Specific intracellular targets of superoxide include ras, aconitase, numerous ion channels and transporters, poly-unsaturated lipids, and many redox-sensitive transcription factors.[1-3] However, a full understanding of how superoxide modulates intracellular signaling and gene expression has been hampered by the lack of potent cell-permeable small-molecule superoxide dismutase (SOD) mimetics. The development of such compounds would provide not only potential therapeutic approaches but also valuable tools to understand the basic biology of ROS and their contribution to pathological states. In the present work we describe the rational design of a new class of SOD mimetics based on malonic acid–derivatized fullerene C_{60} compounds that are cell-and mitochondria-permeable. We used *N*-methyl-D-aspartate (NMDA)-mediated neuronal injury as a model paradigm reported to involve intracellular superoxide to carry out these structure-activity studies.

NMDA receptors are members of the superfamily of ligand-gated ion channels that are involved in several important functions in the central nervous system. It is now known that calcium entry through the NMDA receptor channel plays important roles in development and in forms of synaptic plasticity that may underlie higher order processes such as learning and memory.[4-7] Excitotoxicity associated with overactivation of glutamate receptors, however, has been linked to a number of pathological conditions, ranging from acute insults such as stroke and trauma, to chronic

Received 13 March 2008; accepted 9 May 2008.
This work was funded by a Paul Beeson Physician Scholar Award, the Selma I. Hartke fund for aging research, and NIH NS47966 (L.L.D.).
*Corresponding author. Division of Geriatrics, Department of Medicine, University of California, SCRB/SOM, Mailcode 0746, La Jolla, California, USA 92093-0746.
E-mail address: ssali@ucsd.edu (S.S. Ali).

1549-9634/$ – see front matter © 2008 Elsevier Inc. All rights reserved.
doi:10.1016/j.nano.2008.05.003

Please cite this article as: S.S. Ali, J.I. Hardt, L.L. Dugan, SOD Activity of carboxyfullerenes predicts their neuroprotective efficacy: a structure-activity study. *Nanomedicine: NBM* 2008;4:283-94, doi:10.1016/j.nano.2008.05.003.

neurodegenerative diseases including Huntington's disease, Parkinson's disease, Alzheimer's disease, and amyotrophic lateral sclerosis.[8-11] It has been reported that exposure of neurons to NMDA produces higher levels of ROS, probably through the mitochondrial electron transport chain,[12-15] and previous studies have linked ROS production to NMDA-induced excitotoxic neuronal death.[16-19]

Under physiological conditions, ROS homeostasis is maintained in vivo by the interplay between oxidant production and the antioxidant defense capacity. However, during episodes of oxidative stress, increased free-radical production or reduced antioxidant reserves may shift this balance toward a more pathological state. Because superoxide radical is much less reactive than other ROS, it is sufficiently long-lived to cross cell membranes and reach more vulnerable cellular domains. Consequently, effective targeting of superoxide radical intracellularly is a potentially viable strategy to alleviate pathological conditions attributed to increased oxidative stress. Attempts to develop manganese (Mn)-based SOD mimetics, which can be extremely effective in vitro, were however hampered by the poor membrane penetration of these compounds,[20] whereas nitroxide-based SOD mimetics suffer from very low reactivity toward superoxide[21] and very fast cell clearance.[22]

Fullerenes are three-dimensional carbon networks in which the spherical ring strain forces atoms to undergo partial pyramidalization, therefore imparting them with an increased *s*-orbital character.[23-25] This has been shown to imbue them with metal-like electronic properties[25] and to result in enhanced reactivity of the outer surface of the fullerene derivative toward electron-rich reagents including oxygen free radicals.[26] In a previous report we introduced evidence that supported a catalytic metalloenzyme-like antioxidant activity of the C3 malonic acid C_{60} derivative versus superoxide radical.[26] Our data also suggested that the metal-like properties of fullerene compounds are amenable to targeted modifications to achieve other desirable enzyme-like activities. Indeed, C3 was recently shown by our group to decrease brain oxidative stress and therefore to extend life span of mice when chronically administered in their drinking water[27] while improving their cognitive performance.[28] We have also reported that acute C3 treatment rescues a subset of crucial population of inhibitory interneurons that are lost as a result of induced NADPH oxidase activity—that is, increased superoxide levels in the brain of a schizophrenic model mouse.[29] The present work was carried out to provide insight on the rational design of carboxyfullerenes possessing variable chemical and biophysical properties as tools to study the biology of superoxide and as potential therapeutic candidates to ameliorate disease states resulting from oxidative stress. We therefore establish correlations between the specific antioxidant reactivity of carboxyfullerenes, structural features of the compounds (i.e., number and distribution of malonic acid groups over the C_{60} surface), and their neuroprotective efficacy against NMDA-induced excitotoxicity in cortical neuronal cultures. The structural requirements for neuronal protection by antioxidant strategies are also discussed in terms of in vitro reactivity toward superoxide radical, drug hydrophilicity, and dipole moment, using other benchmark antioxidants for comparison.

Methods

Chemicals

3-morpholino-sydnonimine hydrochloride (SIN-1), cytochrome *c* from bovine heart (cyt c^{III}), SOD from bovine erythrocytes, xanthine, hypoxanthine (HX), xanthine oxidase (XO), and toluene were purchased from Sigma Chemical Co. (St. Louis, Missouri). 2-(4-carboxyphenyl)-4,4,5,5-tetramethylimidazoline-1-oxyl-3-oxide was obtained from Calbiochem (San Diego, California).

Instrumentation

Spectrophotometric measurements were carried out using an Agilent 8453 Ultraviolet (UV)-visible Spectroscopy System (Agilent Technologies, Santa Clara, California) controlled by UV-visible ChemStation Revision A.09.01 software or a Spectramax 190 plate reader (Molecular Devices, Sunnyvale, California), supported by SOFTmax Pro version 3.1.2. All of the high performance liquid chromatography (HPLC) methods used a Hewlett-Packard/Agilent 1100 series HPLC with a quaternary pump and diode array detector. Electron paramagnetic resonance (EPR) experiments were carried out on Bruker Biospin e-scan benchtop spectrometer (Bruker, Biospin, Billerica, Maine).

Preparation of malonic acid and acetic acid C_{60} derivatives

C_{60} was dissolved in toluene and stirred overnight. Dimethyl bromomalonate was then added, followed by 1,8-diazabicyclo (5.4.0) undec-7-ene. The reaction mixture was stirred for 2 hours and filtered through a pad of silica gel; solvent was removed in vacuo. The product was then chromatographed on a silica gel column (280–400 mesh; Merck, Whitehouse Station, New Jersey) using toluene-hexane (1:1 by volume) as eluent. Unreacted C_{60} is eluted first. Various malonic acid C_{60} esters are then eluted sequentially by gradually stepping up the ratio of toluene to hexane (4:1, then 9:1). Each isomer is observable as a colored band on the column, allowing collection of each fraction separately. Finally, toluene with 5% ethyl acetate is then used to elute the band corresponding to C3, followed by three additional derivatives. Purity of the C_{60} malonic ester fractions was monitored by thin-layer chromatography and HPLC. Fractions were evaporated and chromatographed a second time if necessary.

Free acids of the collected esters were then produced by base-catalyzed hydrolysis as described.[28] Esters are dissolved in toluene and purged with nitrogen. Addition of sodium methoxide resulted in precipitation of the corresponding malonic acid products within minutes. The mixture was

stirred continuously at room temperature (22°C–25°C) under nitrogen for 1 hour, and then water was added and the mixture was stirred overnight. The malonic acids partition into the aqueous phase. The layers were separated, and the aqueous layer chilled and acidified with 20% sulfuric acid. The solution was then extracted with ethyl acetate three times, resulting in all product malonic acid C_{60} derivatives going into the organic layer, which was washed several times with water to extract any remaining contaminants. The ethyl acetate was then evaporated and the resulting powder lyophilized to remove residual solvent and water.

To produce P2 or C3lite, C3 was dissolved in acetonitrile-water (1:1) and heated to 60°C to produce sequential mono-decarboxylation of the malonic acids to produce acetic acid groups. After about 1.5 hour of heating the P2 concentration was near maximal, and the reaction was stopped. To obtain C3lite heating was continued for 6 hours. Solvents were removed in vacuo, and the resulting solid products were redissolved in water. To obtain pure P2 or C3lite, the products of thermal decomposition of C3 were separated by preparative HPLC and collected be automated fraction collector. The HPLC was equipped with a Zorbax SB-C18 4.6X250 mm column maintained at room temperature. Solvents were 0.1% trifluroacetic acid (TFA) in water (solvent A) and 0.1% TFA in 95% acetonitrile and 5% water (solvent B). Samples were eluted from the column using a gradient from 40:60 (A/B) to 10:90 (A/B) over 15 minutes, with an additional 15 minutes at 10:90 (A/B). Compounds were monitored and identified by their UV-visible absorbance using an in-line diode array detector. Solvents were then removed in vacuo, and the resulting dry solid product stored at 4°C.

Nuclear magnetic resonance and mass spectroscopy were performed at the Washington University Resource for Biomedical and Bioorganic Mass Spectrometry to confirm identity and purity of the derivatives. Both conventional mass spectrometry with negative-ion analysis (increased sensitivity for negatively charged groups such as carboxylic acids), and electrospray mass spectrometry were used.

Neuronal cell cultures

Neocortical cell cultures were prepared from fetal (E15) Swiss-Webster mice (Simonson, Gilroy, California) as described.[13] Cortical hemispheres were dissected away from the rest of the brain and placed in trypsin (0.25%, Gibco, Carlsbad, California) for 15 minutes. The cortices were briefly centrifuged, the trypsin removed, and the hemispheres resuspended in plating medium, which consists of media stock (Eagle's Minimal Essential Media minus L-glutamine; Gibco 11430-022) with 20 mM glucose, 26.2 mM $NaHCO_3$), 5% fetal calf serum, and 5% horse serum (Hyclone, Logan, Utah) for pure neuronal cultures (<0.5% astrocytes). For neuron-astrocyte co-cultures, the same medium, supplemented with L-glutamine (2 mM) was used. After trituration, cell suspensions were diluted and plated onto a preexisting bed of mouse cortical astrocytes in 24-well Primaria culture plates (Falcon Co., Lincoln Park, New Jersey). Cultures were fed biweekly with growth medium (media stock with 10% horse serum, 2 mM L-glutamine), until the final feeding at day 12, when cultures were fed with media stock supplemented with 2 mM L-glutamine. Cells were used for experiments after 14 to 15 days in culture. All animal studies were approved by the Animal Welfare Committee of the University of California, San Diego, and were in accordance with the PHS Guide for the Care and Use of Laboratory Animals, USDA Regulations, and the AVMA Panel on Euthanasia guidelines.

Injury paradigms

Brief exposure to NMDA was carried out as described.[13] The culture medium was exchanged twice with HEPES–bicarbonate-buffered balanced salt solution, and then NMDA (150 μM) was added alone, or with a C_{60} derivative for 10 minutes. Exposure was terminated by exchanging the medium four times with media stock. The cells were returned to the 37°C (5%) incubator for 24 hours, after which injury was assessed by determination of lactate dehydrogenase (LDH) release,[30] and by visual examination of cultures by bright-field microscopy for degeneration of cell bodies, fragmentation of processes, and development of pyknotic nuclei.

EPR experiments

A Bruker e-scan benchtop EPR spectrometer was used to determine the concentration of superoxide generated through HX-XO metabolism and the scavenging by vitamin E. Mixtures containing variable vitamin E concentration (0–100 μM final) were incubated with XO (0.01 U/mL), HX (85 μM), and 35 mM 5-(diethoxyphosphoryl)-5-methly-1-pyrroline-N-oxide (DEPMPO) for 10 minutes before injection into the EPR cavity of a Bruker e-scan benchtop spectrometer via a Teflon tube with an inner diameter of approximately 0.4 mm. The EPR spectra were recorded using the following setting: receiver gain 1×10^3, scan width 200 G centered at 3484.9 G, modulation amplitude 2 G, time constant 5.16 msec, modulation frequency 86 kHz, microwave power 5.04 mW, 5.24-sec sweep time, and the spectrometer's operating frequency 9.784 GHz. Each spectrum was the average of 10 scans.

Calculations and modeling

Molecular models, geometry optimization, and energy minimization for all molecules were carried out using MM2 force field provided by CS Chem3D Ultra Version 7.0 (CambridgeSoft, Cambridge, Massachusetts) and then verified and refined using CAChe WorkSystem Pro Version 5.04 (Fujitsu America Inc., Sunnyvale, California). Energy minimization of molecules, molecular properties, and electrostatic superdelocalizability potential maps were generated under the Project Manager environment using the following procedures. First, a thorough conformational

search had been carried out within Mechanics using CAChe Augmented MM2 or MM3 parameters through the conjugate gradient method until the gradient was below 0.001 kcal/mol within 3000 steps. Then the unique minimum was fully optimized with MOPAC (PM3 force field). The PRECISE keyword was also used to increase the geometric and electronic convergence criteria. In some cases, the GEO-OK keyword was used to prevent calculation routines from unexpected termination. Finally, an electron-density isosurface map colored by electrostatic potential was accomplished by tabulating at an isosurface value of 0.01 e/Å^3. Calculations for nucleophilic superdelocalizability included solvation effects of water (dielectric constant 78.4 and effective radius of 1.3 Å) simulated by COSMO (Conductor-like Screening Model). Superdelocalizability calculations by CAChe create isosurfaces that display areas in space where the frontier electrons are most likely to be found, depending on the attacking reagent energy. A good value for the reagent energy is one which is lower than the LUMO energy of the substrate and which approximates the energy of the reagent's frontier orbital. A value of −5 eV was estimated for the superoxide anion through energy level calculations using CAChe (Fujitsu America Inc.). Same procedure was applied to obtain the nucleophilic superdelocalizability of α-tocopherol.

Molecular docking studies of the native ligands and carboxyfullerenes into the binding pockets in NR1 and NR2A subunits of the NMDA receptor were carried out using the BioMedCAChe suite of algorithms. The x-ray structure of the ligand-binding core of the NR1-NR2A heterodimer subunit at 2.0-Å resolution in complex with glycine and glutamate was downloaded from the Protein Data Bank website(http://www.rcsb.org/, entry 2A5T).[31,32] After correcting the crystal structure of NR1-NR2A protein complex for valency and hydrogen bonding, glycine or glutamate were re-docked into their identified pocket (defined to include all atoms and groups within 7 Å radii of the co-crystallized ligands) by holding the residues of the protein fixed and allowing the ligand to be flexible. The orientation and hydrogen bonding of the re-docked complex were close to that in the crystal structure, and the flexibility of the protein residues of the active site was consequently allowed. The docking scores were then calculated using a genetic algorithm (1500 generations) with a fast, simplified potential of mean force (grid spacing 0.3 Å). Native ligands were subsequently replaced with each of the studied carboxyfullerenes or known competitive inhibitors in the respective binding sites, and the docking scores were evaluated using the routine described above.

Results

Structures of carboxyfullerenes used in this study

In Figure 1 we provide the structural models of all of the six compounds used in the present study. These models were generated as described in the "Calculations and Modeling" section above. The selection of these compounds was based on structural variability that illustrates the functional dependence on two molecular structural aspects. First, the number of carboxylic acid groups attached to the fullerene moiety was increased from three to six in the order C3lite< bisE< P2< C3; second, the distribution of a fixed number of carboxylic groups over the fullerene was varied in the hexacarboxylic acid isomers (C3, E, and D3).

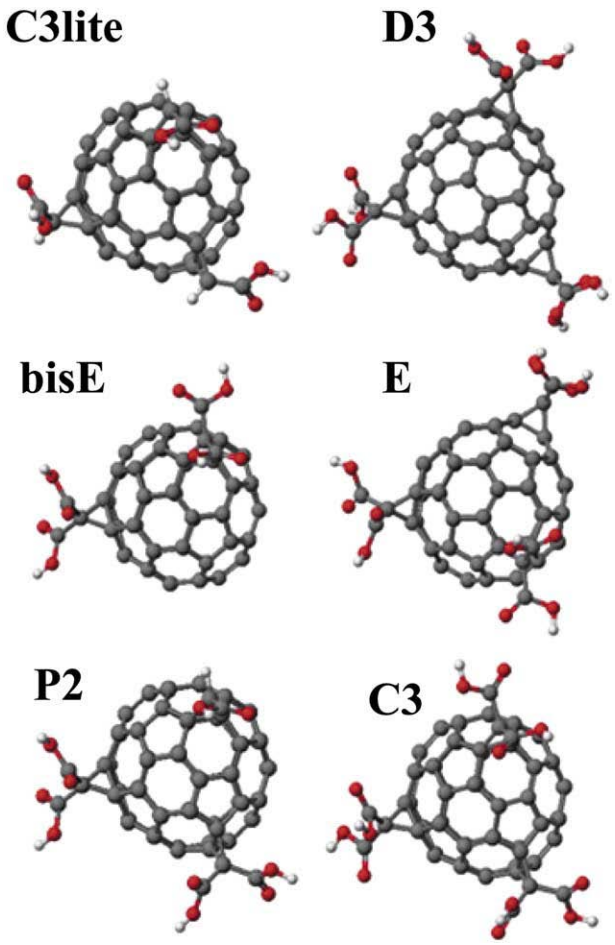

Figure 1. Structural models of the carboxyfullerenes used in the present study. Molecular models, geometry optimization, and energy minimization for all molecules were carried out to arrive at the indicated structural models. The selection of these compounds was based on structural variability that illustrates the functional dependence on two molecular structural aspects: First, the number of carboxylic acid groups attached to the fullerene moiety was increased from three to six in the order C3lite < bisE < P2 < C3; second, the distribution of a fixed number of carboxylic groups over the fullerene surface was varied in the hexa-isomers (C3, E, and D3). The IUPAC nomenclatures of these compounds are: **bisE**, 3′*H*,3′′*H*-dicyclopropa[1,9:21,40]-(C_{60} I_h)[5,6][fullerene-3′,3′,3″,3″-tetracarboxylic acid; **C3lite**, 3′*H*,3″*H*,3‴*H* tricyclopropa[1,9:21,40:44,45]-(C_{60}-I_h)[5,6]fullerene-3′,3″,3‴-tricarboxylic acid; **P2**, 3′*H*,3″*H*,3‴*H*-tricyclopropa[1,9:21,40:44,45]-(C_{60}-I_h)[5,6]fullerene-3′,3′,3″,3″,3‴-pentacarboxylic acid; **E**, 3′*H*,3″*H*,3‴*H*-tricyclopropa[1,9:21,40:34,35]-(C_{60}-I_h)[5,6]fullerene-3′,3′,3″,3″,3‴,3‴-hexacarboxylic acid; **C3**, 3′*H*,3″*H*,3‴*H*-tricyclopropa[1,9:21,40:44,45]-(C_{60}-I_h)[5,6]fullerene-3′,3′,3″,3″,3‴,3‴-hexacarboxylic acid; **D3**, 3′*H*,3″*H*,3‴*H*-tricyclopropa[1,9:34,35:43,57]-(C_{60}-I_h)[5,6]fullerene-3′,3′,3″,3″,3‴,3‴-hexacarboxylic acid.

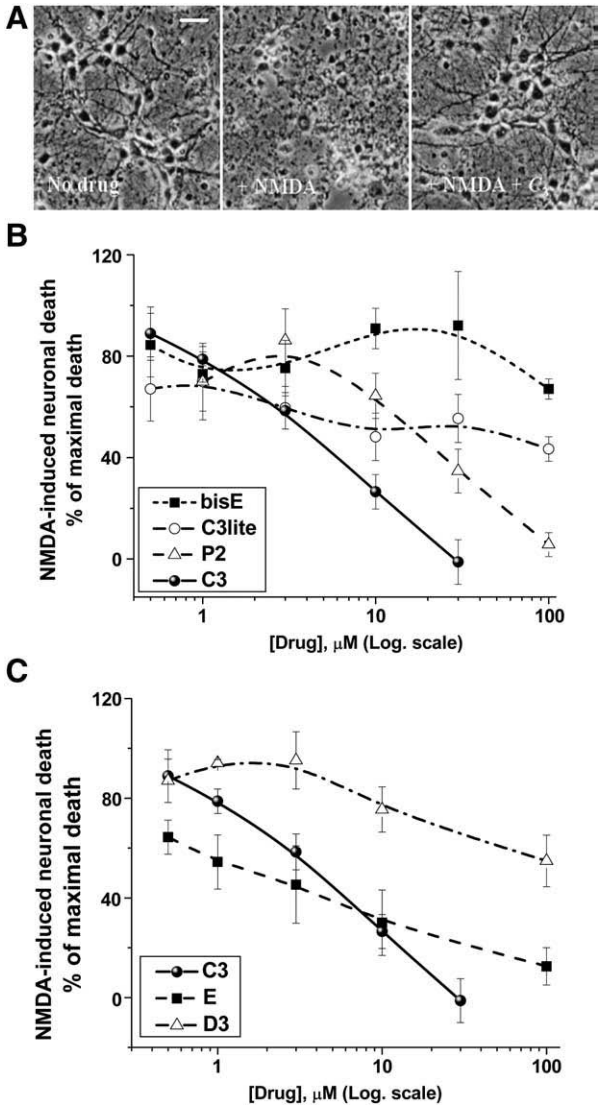

Figure 2. Neuroprotection by carboxyfullerenes in NMDA receptor–mediated excitotoxic injury. Neurotoxicity produced by exposure to NMDA is reduced by co-application of the carboxyfullerenes. Data are presented as the percentage of cell death (LDH release) produced by NMDA alone, mean ± SEM, $n > 12$. **(A)** Phase-contrast images of cultured cortical neuronal 24 hours after drug exposure; control (left), NMDA (middle), NMDA plus 30 μM C3 (right). **(B)** Increasing the number of carboxylic group on the C_{60} surface increases neuronal survival, with the exception of the bisE compound (reviewed in more detail in the Discussion). **(C)** Neuronal protection provided by carboxyfullerenes that possess the same number of carboxylic groups but differ in their distribution over the C_{60} sphere; see the structures in Figure 1. The white bar is 25 μm.

Neuroprotective efficacy of carboxyfullerenes against NMDA toxicity in cortical neurons

To evaluate the effect of different carboxyfullerenes on NMDA receptor–mediated excitotoxicity, mouse cortical neuronal cultures were exposed to 150 μM NMDA for 10 minutes, with cell death assayed 24 hours later. Carboxyfullerenes were included only during the period of NMDA exposure. This is a commonly used paradigm to study excitotoxic neuronal injury through NMDA receptors, and to probe downstream events that contribute to the excitotoxic cascade. Figure 2 shows neuroprotection by C3 at 30 μM, demonstrated by bright-field photomicrographs 24 hours after NMDA exposure (Figure 2, *A*), and by cell death as assayed by LDH release from degenerating neurons (Figure 2, *B*, *C*). By constructing dose-protection curves for all compounds, it was concluded from Figure 2, *B* that increasing the number of carboxylic groups enhances neuroprotective efficacy. That is, whereas 30 μM C3 (six carboxylic groups) was sufficient to completely block neuronal death, concentrations of up to 100 μM of C3lite (three carboxylic groups), bisE (four carboxylic groups), and P2 (five carboxylic groups) only partially blocked NMDA-mediated neuronal death. Neuroprotection was also dependent on the symmetry of distribution of the carboxylic groups over the C_{60} core (Figure 2, *C*), with more clustered malonic acid groups conferring better neuroprotection, in general. Values for the half-maximal inhibitory concentration (IC_{50}), and the concentrations at which each carboxyfullerene compound provided maximal neuroprotection are given in Table 1. Values for α-tocopherol, the metalloporphyrin, MnTMPyp, and the spin-trap phenylbutyl nitrone, are included for comparison. Data in Figure 2 and Table 1 indicate that C3, E, and P2 are much more potent neuroprotective compounds than bisE, C3lite, and D3, and that all are more potent and effective than three commonly-used antioxidants, α-tocopherol, MnTMPyp, and phenylbutyl nitrone.

Table 1
Comparison of the efficacy of carboxyfullerene isomers with other commonly studied antioxidants

Drug	IC_{50} (μM)	Percentage maximum achievable protection [μM]
C3lite	10	66 [10]
BisE	>100	43 [100]
P2	17	93 [100]
C3	4	100 [30]
E	9	87 [100]
D3	>100	46 [100]
α-Tocopherol	>100	22 [100]
MnTMPyp	>100	16 [50]
Phenylbutyl nitrone	>100	15 [300]

Mixed cortical cultures were exposed to NMDA for 10 minutes in the presence of antioxidant compounds, and cell death was assessed at 24 hours by LDH release. A range of concentrations for each antioxidant was tested; the maximal protection and the concentration at which it was achieved are listed. Values are expressed as percentage of NMDA-induced death in the absence of test compound.

Efficacy of the different carboxyfullerenes against superoxide radical in vitro

A direct implication of the neuroprotection pattern observed with different carboxyfullerenes is that it seems

to require not only an increasing number of carboxylic acid groups, but also specific positioning of these groups on the fullerene surface. In a previous article we reported that C3 is a potent antioxidant that eliminates superoxide radical catalytically.[26] Therein we suggested a mechanism in which C3 facilitates the superoxide dismutation through electrostatic stabilization of the negatively charged superoxide on electron-deficient regions of C3 in coordination with the carboxylic acid groups. Here we attempt to evaluate and compare the efficacy of the different malonic acid derivatives as superoxide-eliminating antioxidants. In doing this, our goal was to explore the structural criteria that may dictate the potency of a particular carboxyfullerene as an antioxidant in vitro and to eventually establish a correlation with its efficacy as a neuroprotective compound in neuronal cell culture.

Based on the observation that dismutation of superoxide by C3 is catalytic and is not due to direct scavenging of $O_2^{\cdot-}$, we attempted to model the interaction between superoxide and each compound used in this study. Semi-empirical quantum-mechanical calculations were carried out to predict the electron distribution on the surface of each compound and for α-tocopherol as a control antioxidant. The mapping depicted in Figure 3 indicates the nucleophilic superdelocalizability contour, which is a measure of the susceptibility of each fullerene derivative to be attacked by a nucleophile (superoxide anion in this case). Each contour in Figure 3 can be seen as a qualitative indicator of the reactivity of the molecule toward $O_2^{\cdot-}$, which is electrostatically driven toward electron-deficient areas on the C_{60} surface (white/red regions, Figure 3). One should therefore expect that the larger the white/red regions on the C_{60} surface, the more reactive the molecule toward superoxide radical will be. The carboxyl groups are important because they can stabilize $O_2^{\cdot-}$ by hydrogen bonding until a second $O_2^{\cdot-}$ arrives to combine with the original $O_2^{\cdot-}$, allowing dismutation of $O_2^{\cdot-}$ with the help of protons from the carboxyl groups and/or local water molecules. In Figure 3, and for the sake of comparison, we also provide the superdelocalizability map for α-tocopherol. It seems that, in terms of the electrostatic drive, α-tocopherol is much less reactive toward superoxide radical relative to any of the studied carboxyfullerenes. This finding is important because, although α-tocopherol is clearly a highly effective chain-breaking lipid peroxidation inhibitor (10^6 $M^{-1}s^{-1}$),[33] its low reactivity toward superoxide and lack of significant neuroprotective efficacy against NMDA supports the concept that superoxide elimination is key to neuroprotection.

The maps in Figure 3 confirm that regions around the malonic acid groups are the most electron-deficient areas and are therefore electrostatically attractive for the approaching superoxide anion. Charge distribution is however sensitive to the symmetry of each molecule as expected. As a result, the highest symmetry of the D3 hexa-isomer is associated with the least electronic detraction as a result of opposing charge withdrawal by equivalent malonic groups. In the case of C3 it is reasonable to conclude that the maximum number of malonic acid groups that are clustered in the vicinity of each other on the C_{60} surface optimizes electronic, steric, as well as topological conditions to eliminate $O_2^{\cdot-}$ according to the proposed mechanism. It is important to note that the neuroprotective efficacies of the studied drugs (Figure 2 and Table 1) qualitatively correlate with their superoxide affinity trend except in the case of bisE, which exhibits weak neuroprotection while seeming to possess widely spread electron-deficient regions. This anomaly can however be understood if we consider the factor of solubility of bisE as discussed below.

Kinetics and pH dependence of superoxide elimination by carboxyfullerenes

Next, we assayed the in vitro reactivity of each carboxyfullerene and of α-tocopherol toward $O_2^{\cdot-}$. To determine the kinetics of the reactions of different carboxyfullerenes with superoxide anion in vitro, $O_2^{\cdot-}$ was generated enzymatically through XO metabolism of HX. The concentration of $O_2^{\cdot-}$ was determined using a microplate assay,[34] based on the SOD-inhibitable reduction of ferricytochrome c,[35] and followed as absorbance at 550 nm.[26–34] To confirm that carboxyfullerenes do not inhibit XO activity, we measured both purine metabolites and O_2 consumption during the reaction, and observed that even at 300 μM, C3 inhibited XO by less than 10%.

The solubility of fullerenes is strongly dependent on the number of carboxylic groups and hence on the pH of the working solutions. Consequently, and to enhance the solubility of less hydrophilic compounds, we used thermal decomposition of SIN-1 as a second method to generate superoxide at higher pH values (8.5–10.5)[26]; the results are shown in Figure 4, *A–C*). The SIN-1 system provides another advantage, in that the decomposition of SIN-1 is controllable by both pH and temperature. This allowed control of the rate of superoxide generation and hence enabled us to perform kinetic and mechanistic studies at variable temperatures and pH values. Kinetic analyses and determination of k_i and IC_{50} values were carried out as described earlier.[25]

A representative dose-response curve at pH 7.4 (phosphate-buffered saline, HX-XO system) in the case of C3 is given in Figure 4, *A*, along with curves obtained using the SIN-1 system in glycine-sodium hydroxide buffer adjusted to pH values of 8.5, 9, 9.5, and 10. Similar curves obtained for D3 at pH values of 9, 9.5, and 10 are provided in Figure 4, *B* to confirm that these compounds react with superoxide through the same mechanism. It is clear from Figure 4 (*A*, *B*) that carrying out the reaction at lower pH values was associated with systematic increases in the efficacy of the drug in removing superoxide as marked by decreased IC_{50} values. In fact we observed an order of magnitude increase in the rate constant of the carboxyfullerene-superoxide reactions when the pH of the reaction

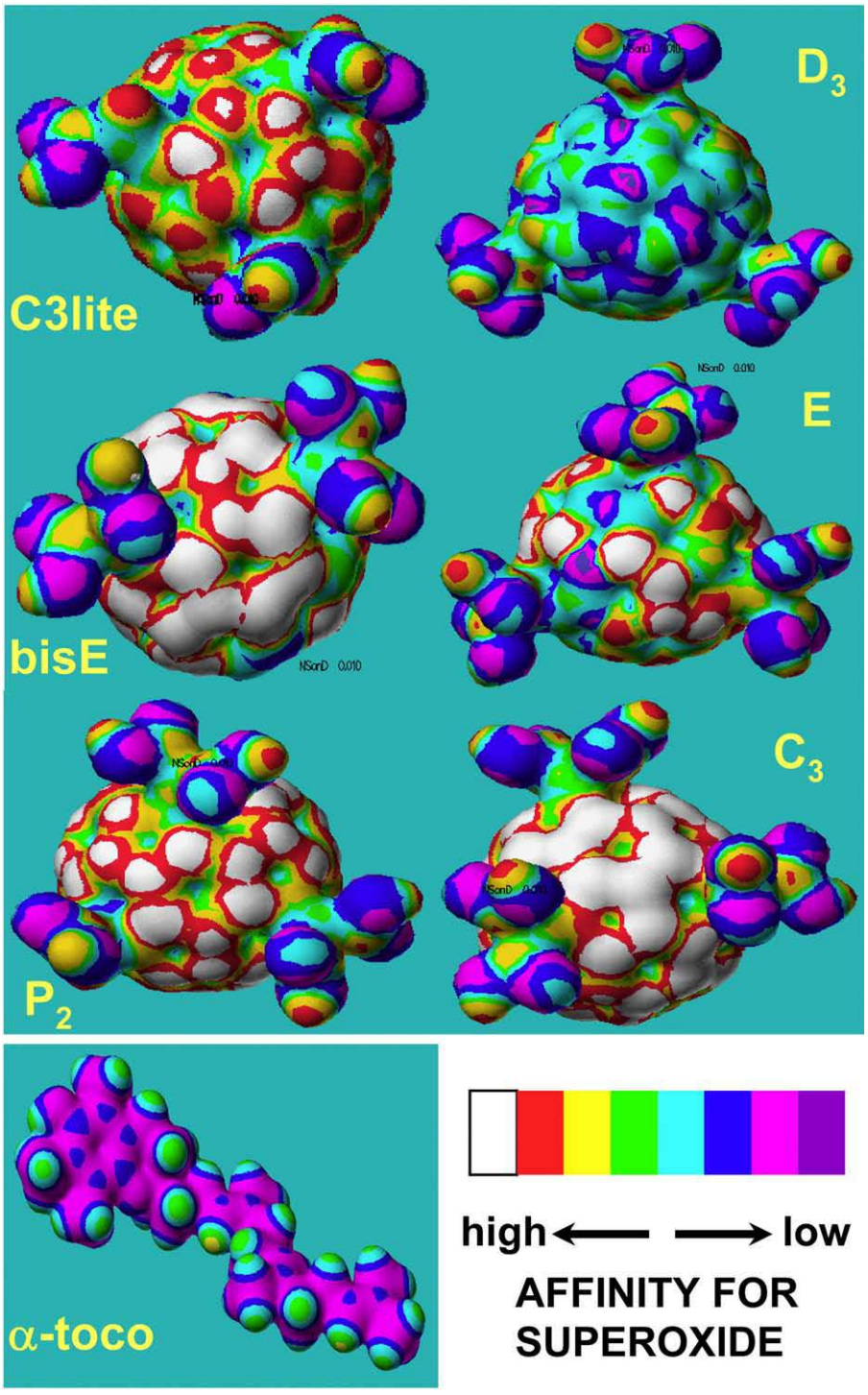

Figure 3. Nucleophilic superdelocalizability maps for carboxyfullerenes and vitamin E. Electron-density mapping reflects nucleophilic superdelocalizability indicating on the resulting isosurface locations that are susceptible to attack by superoxide, and designated by a color scale showing decreasing susceptibility in the order white through cyan (see legend).

medium was reduced by one unit. This relation was independent on the source of superoxide used and was more pronounced in the case of the hexa-isomers (Figure 4, *C*) indicating the importance of shifting the carboxylic groups toward their neutral acid form as a prerequisite to augment the reactivity of the molecule against superoxide anion. Taken together, these observations support the suggested catalytic dismutation of superoxide by carboxyfullerenes, which seem to follow a similar mechanism albeit with different reactivity and hence variable kinetics.

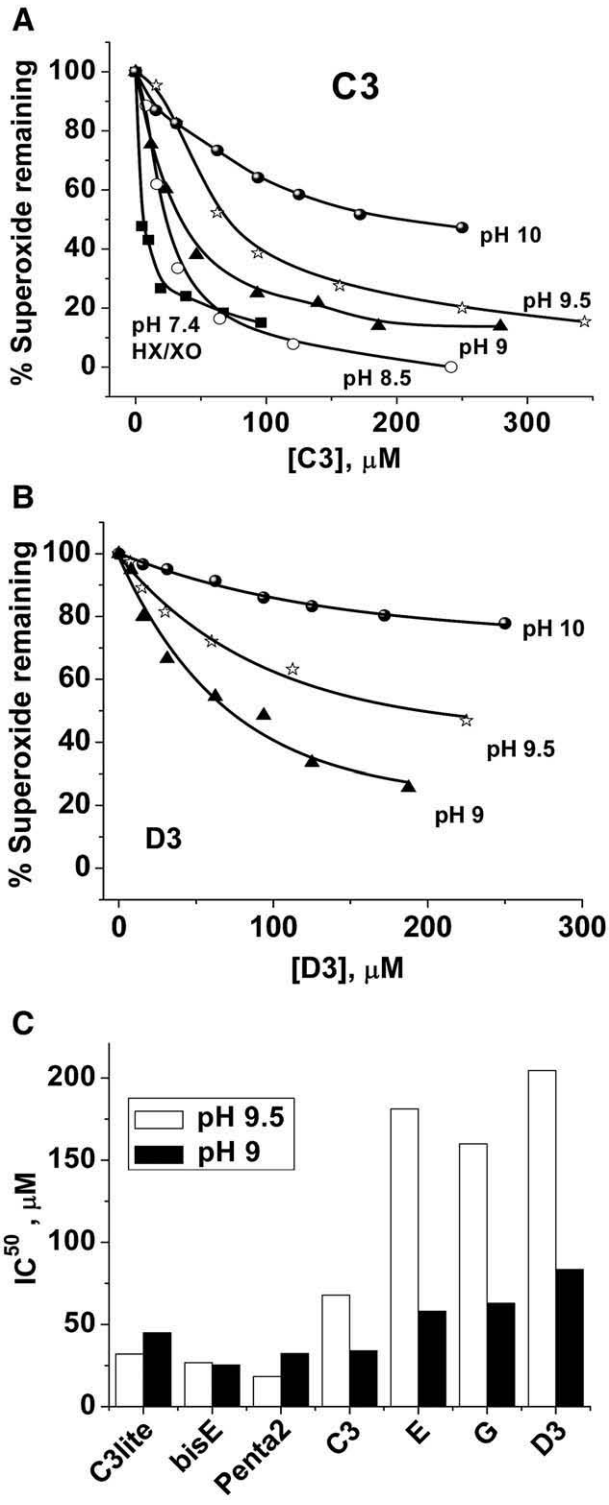

Figure 4. Carboxyfullerenes eliminate superoxide faster at lower pH. C3 shows an order of magnitude faster rate of superoxide elimination as compared to D3. Compare (**A**) and (**B**). Both drugs showed an inverse relationship between the efficiency of superoxide removal and pH; a trend that was more pronounced in the hexa isomers as shown in (**C**). Superoxide was generated by HX-XO metabolism at pH 7.4, or through thermal decomposition of SIN-1 at pH values of 8.5, 9.0, 9.5, and 10. See experimental section for details.

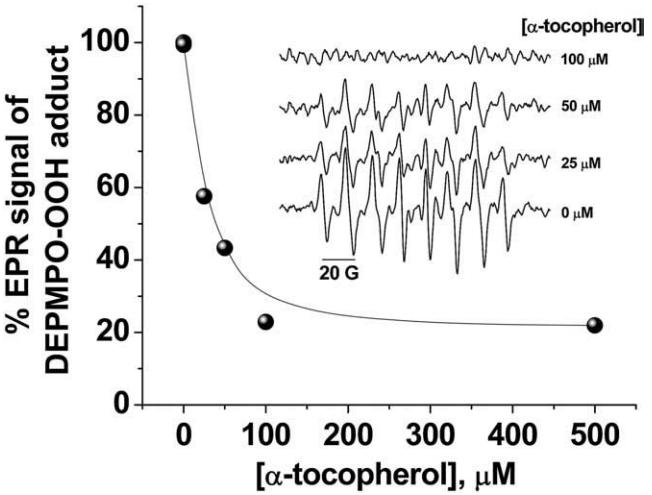

Figure 5. Kinetics of superoxide elimination by α-tocopherol. The effect of increasing the concentration of α-tocopherol from 0 to 100 μM on the EPR signal from the DEPMPO-superoxide spin adduct is shown. Superoxide was generated by HX-XO metabolism and measured by EPR spectroscopy using the spin-trap, DEPMPO. EPR settings were: receiver gain 1×10^3, scan width 150 G centered at 3484.9 G, modulation amplitude 2 G, time constant 5.16 msec, modulation frequency 86 kHz, microwave power 5.04 mW, 5.24-sec sweep time, and the spectrometer's operating frequency 9.784 GHz. Each spectrum was the average of 10 scans. The rate constant for the reaction between superoxide and α-tocopherol is $k_{\alpha\text{-toco}} = 6.0 \times 10^4\ M^{-1}s^{-1}$.

We also carried out a spin-trapping competitive EPR experiment to determine the rate constant of superoxide removal by α-tocopherol, and the results are given in Figure 5. Other assays for superoxide determination such as those dependent on optical methods, including cyt c^{III} assay and fluorescence readouts, are not accurate in this case because of turbidity artifacts caused by the lipophilic α-tocopherol when mixed with the aqueous assay medium. In this experiment, superoxide radical was generated by HX-XO system in phosphate-buffered saline at pH 7.4 in the presence of 35 mM DEPMPO, and the reaction mixture was incubated for 20 minutes at 25°C with different concentrations of α-tocopherol (0–100 μM). When competitive kinetics were applied on the results obtained through Figure 5 and using the reported k_{DEPMPO} range of values of 4 to 58 $M^{-1}s^{-1}$ (ref.[36]), $k_{\alpha\text{-toco}}$ was calculated to be in the range 0.35×10^4 to $5.8 \times 10^4\ M^{-1}s^{-1}$ versus superoxide. This is comparable with the value, for example, of $k_{\alpha\text{-toco}} = 4.9 \times 10^3\ M^{-1}s^{-1}$ obtained for α-tocopherol incorporated into soybean and dimyristoyl phosphatidylcholine liposomal membranes.[37] We will use the upper limit of the estimated $k_{\alpha\text{-toco}}$ approximately $6 \times 10^4\ M^{-1}s^{-1}$ against superoxide to compare with carboxyfullerenes in the Discussion section.

Carboxyfullerenes do not bind to the glutamate or glycine binding sites on the NMDA receptor: molecular docking calculations

We have previously reported that application of C3 or D3 along with NMDA does not decrease NMDA-stimulated $^{45}Ca^{2+}$influx into cultured neurons and does not reduce the

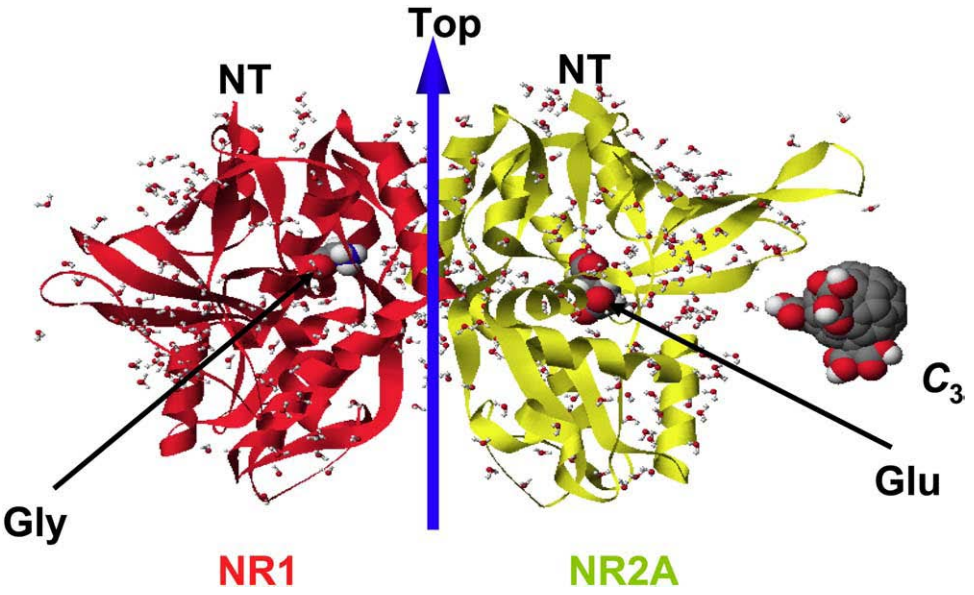

Figure 6. Carboxyfullerenes do not compete with the native ligands of the NMDA receptor. Side view of the NR1-NR2A S1S2 heterodimer in complex with glycine (left) and glutamate (right). As a representative carboxyfullerene, C3 was placed by the protein to illustrate the size of carboxyfullerenes in comparison with that of the native ligands. Although the calculated binding scores for native ligands and known competitive agonists-antagonists were exothermic and therefore favorable, those for all carboxyfullerenes were highly unfavorable; see text for additional details.

immediate neuronal swelling induced by NMDA,[19,38] as would be expected by blockade of the NMDA receptor directly. However, to further eliminate the possibility of direct ion channel regulation by carboxyfullerenes, we examined the binding of all compounds in the glutamate and glycine active sites of the NR1 and NR2A subunits of the NMDA receptor and found that this binding is energetically unfeasible due to highly destabilizing steric blocking between the protein and carboxyfullerenes (Figure 6). To validate our findings we calculated the docking scores for the native ligands—that is, glycine and glutamate, in their respective binding sites and those for their reported competitors NMDA, D-AP5, D-serine, and ACPC.[38] All of these compounds exhibited stabilizing interactions in their defined binding pockets as revealed by their exothermic binding scores, which indicate that our calculations can accurately predict the binding affinity of carboxyfullerenes. The calculated docking scores in kilocalories per mole were: glutamate, −69.3; NMDA, −76.8; D-AP5, −76.2; glycine, −27.6; D-serine, −46.0; ACPC, −16.6; carboxyfullerenes (all compounds) > +500. Taken together with our previous results, the current molecular docking calculations support the conclusion that the rescue from NMDA-induced neuronal death by carboxyfullerenes is not due to NMDA receptor blockade.

Reactivity toward superoxide and bioavailability determine neuroprotection

The results in Figures 2 through 4 and Table 1 indicate that both the number of carboxylic groups and their distribution are important in determining the efficacy of the drug. In Figure 7 we compare neuroprotective efficacy, the calculated dipole moments as indicators for reactivity trend toward superoxide, the in vitro rates of elimination of superoxide, and expected rate of cellular drug uptake based on their partition coefficients. It can be seen from Figure 7 that, with the exception of bisE, the neuroprotective efficacy increases with the number of carboxylic groups, moving from C3lite to C3. Although somewhat similar trends for both dipole moment and k_i values were observed, we believe that more significant correlations between these parameters may be modified by other factors, such as rate of cellular uptake. Although the overall performance of each drug, including α-tocopherol, can be qualitatively explained in terms of these parameters, bisE represented an exception, in that it showed the maximum k_i for superoxide, but less neuroprotection than expected. Its low hydrophilicity is expected to slow its ability to enter cells, and therefore, this anomaly may reflect lack of uptake into cells during the very brief (10-minute) exposure time.

When the number of carboxylic groups is kept constant in the hexa-isomer series, the hydrophilicity (inverse partition coefficient) was also constant as seen in the upper panel of Figure 7. Under this structural constraint, the correlation between neuroprotection and the efficacy toward superoxide followed a clear decreasing trend in the order C3> E> D3. In this particular order, the drug's nucleophilic superdelocalizability maps clearly show decreased reactivity toward superoxide (Figure 3), the dipole moment decreases, and the kinetics of superoxide removal become slower, whereas neuroprotection drops from 100% by C3 to 50% by E to virtually no protection by D3 at 30-μM doses (Figure 7).

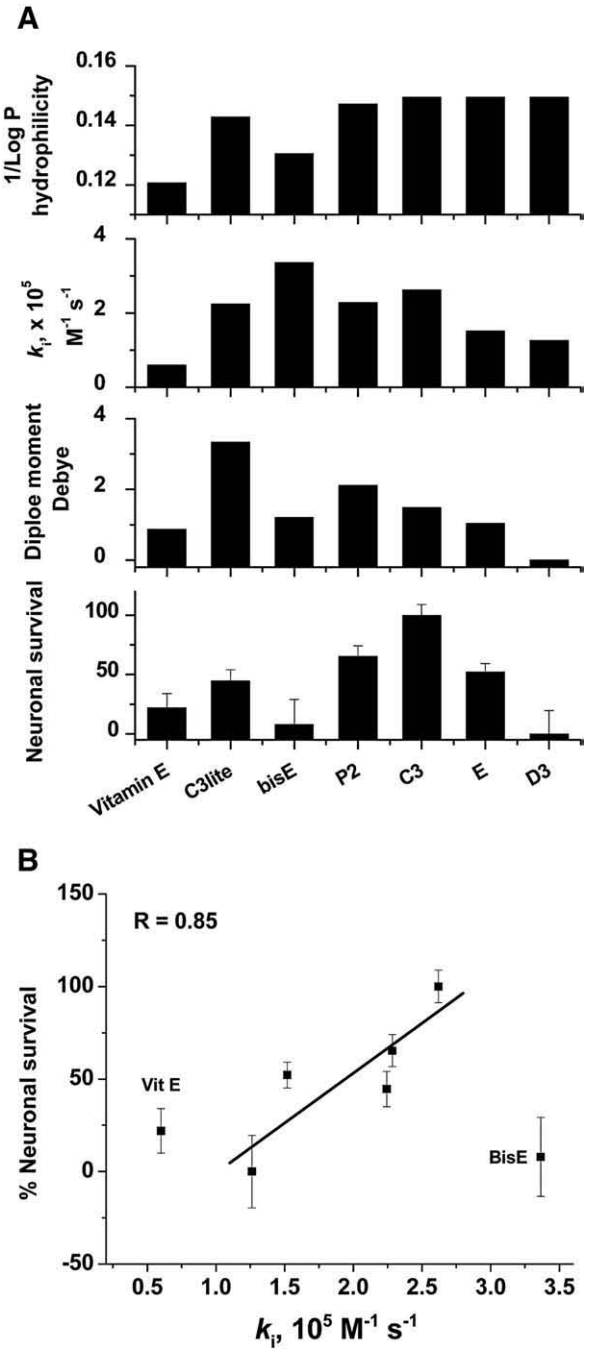

Figure 7. A, Correlation between rescue from NMDA-induced neuronal death and calculated dipole moment, experimentally determined rate of superoxide elimination, and calculated hydrophilicity for each drug at 30 μM (100 μM in the case of α-tocopherol). Maximum protection shown by the C3 isomer is consistent with it having optimal hydrophilicity, symmetry, and a high rate of superoxide elimination. Although the overall performance of each drug, including α-tocopherol, can be qualitatively explained in terms of the parameters, bisE represented an exception, in that it showed the maximum k_i for superoxide, but less neuroprotection than expected. Its low hydrophobicity is expected to slow its ability to enter cells, and therefore, this anomaly may reflect lack of uptake into cells during the brief (10 minutes) exposure time. B, Regression analysis indicates a good correlation (R = 0.85) between neuroprotective efficacy and k_i for superoxide across isomers, with the exception of bisE, whose low aqueous solubility counterbalances its high k_i. α-tocopherol is also included for comparison.

Discussion

The goals of the current study were three-fold: (1) to determine the structural requirements for neuronal protection by antioxidant strategies vis-à-vis in vitro reactivity toward superoxide radical, drug hydrophilicity, and dipole moment, using several benchmark antioxidants as references; (2) to determine whether neuroprotection against NMDA toxicity correlated with and was predicted by the $k_{\text{i-superoxide}}$ of the compounds; and finally (3) to provide a versatile panel of water-soluble, cell-permeable SOD mimetics, supported by structure-activity data, as tools to investigate the biology of superoxide more broadly.

NMDA receptor-mediated neurotoxicity is implicated in many human disease states including trauma, ischemia, epilepsy, and chronic neurodegenerative disorders such as Alzheimer's disease, Parkinson's disease, and amyotrophic lateral sclerosis. Excitotoxicity due to NMDA receptor overactivation can result in excess elevation of intracellular calcium and activation of subsequent events that lead to neuronal death.[39,40] Although NMDA-receptor antagonists prevent neuronal injury in cellular and animal models, in humans their side effects, including nausea, vomiting, and memory impairment, have removed them as viable candidates for clinical applications.[41]

Studies have shown that overactivation of NMDA receptors leads to oxidative stress, and compounds that possess antioxidant properties protect against NMDA neurotoxicity, although subsequent work on many of these compounds indicate that they may act through non-antioxidant mechanisms. One such study on the metalloporphyrin class of SOD mimetics indicated that neuroprotection by these potent antioxidant compounds does not correlate with their SOD activity,[20] and that compounds that had no antioxidant properties were also protective. Neuroprotection was attributed to the ability of the metalloporphyrins to limit delayed calcium dysregulation after NMDA receptor overactivation. Because this study also indicated that these compounds did not enter cells during the exposure period (30 minutes), the authors concluded that metalloporphyrins functioned at the plasma membrane to suppress intracellular Ca^{2+}increases following NMDA receptor activation, and not through their actions as SOD mimetics. However, that these compounds, though potent SOD mimetics, were not cell-permeable revives the question of whether increased intracellular superoxide levels are critical to NMDA receptor-mediated injury.

In the present article we wanted to establish the criteria for an optimized carboxyfullerene antioxidant and to determine whether the observed neuroprotection is due to the elimination of superoxide radical. A set of six different carboxyfullerenes was synthesized, and their reactivity against superoxide radical was studied theoretically as well as experimentally. In the selected compounds we varied the functionalization to follow the dependence of reactivity on an increasing number of carboxylic acid groups attached to

the fullerene moiety in the order C3lite< bisE< P2< C3, and the distribution of a fixed number of carboxylic groups over the fullerene ball in the hexa-carboxylic isomers (C3, E, and D3).

We observed a significant correlation between the neuroprotective efficacy of different carboxyfullerenes and their SOD activities (k_i). Neuroprotection also correlated with the dipole moment. A clear exception to both of these is the bisE compound, discussed further below. The dipole moment is a property we previously suggested to be important to superoxide elimination by carboxyfullerenes based on electrostatic interaction between superoxide and the compound.[26] The high degree of correlation between neuroprotection and these two parameters, both of which predict efficacy as SOD mimetics, provide strong support for the view that superoxide radical contributes to NMDA receptor-mediated neurotoxicity. In addition to SOD activity, biophysical properties that predict the ability of compounds to enter and distribute throughout cells were also found to be associated with improved neuroprotection. The compounds that best highlight this relationship are C3lite, bisE, and C3, which show neuroprotection in the rank order C3> C3lite> bisE. Based on their k_i values against superoxide alone, however, one would expect that neuroprotection would be in the order bisE> C3> C3lite. bisE is the least hydrophilic compound (other than α-tocopherol) and is predicted to have lower water solubility than the other carboxyfullerenes (confirmed experimentally). We have previously reported that the C3 and D3 compounds, which are actually less lipophilic than both the bisE and C3lite compounds, can intercalate into lipid bilayers.[19] Studies using an anti-C_{60} antibody and western blot analysis[42] or immunocytochemistry[26] to detect C3 have shown rapid uptake and intracellular distribution of C3 into neurons, and specifically into mitochondria.[26,42] Based on this, we believe that the bisE compound probably becomes "trapped" in the plasma membrane, with limited transfer into the more aqueous cell interior. C3lite, which also has a lower 1/Log P than C3, may likewise have slower uptake into intracellular compartments. Thus, the rate and degree of cell permeability may be optimized at a 1/Log P of approximately 0.15 and probably modifies the predicted neuroprotective efficacy of the carboxyfullerenes based on their SOD mimetic activities alone. Of note, we interpreted the lack of significant neuroprotection provided by α-tocopherol to suggest that lipid peroxidation, though an observed consequence of NMDA receptor overactivation, may be downstream of the point at which cells can be effectively rescued.

The C3 and D3 compounds have been shown to be neuroprotective in a range of in vitro injury models, including many that do not involve the NMDA receptor,[19,43] and they did not block NMDA-stimulated $^{45}Ca^{2+}$influx.[19] Moreover, C3 compound, administered long term to mice, not only extended life span[27,28] but improved spatial learning and memory performance on the Morris water maze,[28] a task that is quite sensitive to NMDA receptor inhibition. However, to further confirm that neuroprotection was not through direct antagonism at either the glutamate-or glycine-binding sites, we carried out molecular docking calculations for all carboxyfullerenes and found that binding was sterically prohibited and thermodynamically highly unfavorable at both binding sites, as shown in Figure 6.

In summary, molecular modeling and in vitro studies have been used to arrive at an optimum compromise between the SOD activity of carboxyfullerenes and their biophysical properties, and correlations between these parameters and neuroprotective efficacy were then established. Chemical features that enhanced the biological effectiveness of a carboxyfullerene included maximum number of carboxylic groups that are distributed as close to each other as possible, largest dipole moment, and significant solubility in water. Based on these factors, the C3 compound would be predicted to provide the greatest degree of neuroprotection, as was observed experimentally. Taken together, our results indicate that developing SOD mimetics with a high k_i for superoxide, moderate dipole moment, and a balance between lipophilic and hydrophilic properties (i.e., 1/Log P of ~0.15–0.16) may be an attractive strategy for drug development for disease and injury conditions in which superoxide is involved. We believe these data also provide strong support for the idea that superoxide is an important downstream mediator of neurotoxicity triggered by NMDA receptors. Further studies should provide insights into how superoxide interacts with delayed calcium dysregulation and other pathways implicated in NMDA receptor-mediated neuronal injury. Finally, our results indicate that the malleability of fullerenes to functionalization can confer selected biological properties and biophysical characteristics, giving this class of molecules a unique ability to be adapted or tailored for specific biological applications and molecular targets.

References

1. Finkel T. Oxidant signals and oxidative stress. Curr Opin Cell Biol 2003;15:247-54.
2. Liu H, Colavitti R, Rovira II, Finkel T. Redox-dependent transcriptional regulation. Circ Res 2005;97:967-74.
3. McCord JM, Edeas MA. SOD, oxidative stress and human pathologies: a brief history and a future vision. Biomed Pharmacother 2005;59: 139-42.
4. Maren S, Baudry M. Properties and mechanisms of long-term synaptic plasticity in the mammalian brain: relationships to learning and memory. Neurobiol Learn Mem 1995;63:1-18.
5. Asztely F, Gustafsson B. Ionotropic glutamate receptors. Their possible role in the expression of hippocampal synaptic plasticity. Mol Neurobiol 1996;12:1-11.
6. Nakanishi S. Molecular diversity of glutamate receptors and implications for brain function. Science 1992;258:597-603.
7. Nakanishi S, Nakajima Y, Masu M, Ueda Y, Nakahara K, Watanabe D, et al. Glutamate receptors: brain function and signal transduction. Brain Res Brain Res Rev 1998;26:230-5.

8. Brauner-Osborne H, Egebjerg J, Nielsen EO, Madsen U, Krogsgaard-Larsen P. Ligands for glutamate receptors: design and therapeutic prospects. J Med Chem 2000;43:2609-45.
9. Dingledine R, Borges K, Bowie D, Traynelis SF. The glutamate receptor ion channels. Pharmacol Rev 1999;51:7-61.
10. Choi D. Antagonizing excitotoxicity: a therapeutic strategy for stroke? Mt Sinai J Med 1998;65:133-8.
11. Beal MF, Howell N, Bodis-Wollner I. Mitochondria and free radicals in neurodegenerative diseases. New York: John Wiley and Sons; 1997.
12. Reynolds IJ, Hastings TG. Glutamate induces the production of reactive oxygen species in cultured forebrain neurons following NMDA receptor activation. J Neurosci 1995;15:3318-27.
13. Dugan LL, Sensi SL, Canzoniero LM, Handran SD, Rothman SM, Lin TS, et al. Mitochondrial production of reactive oxygen species in cortical neurons following exposure to *N*-methyl-D-aspartate. J Neurosci 1995;15:6377-88.
14. Bindokas VP, Jordan J, Lee CC, Miller RJ. Superoxide production in rat hippocampal neurons: selective imaging with hydroethidine. J Neurosci 1996;16:1324-36.
15. Sengpiel B, Preis E, Krieglstein J, Prehn JH. NMDA-induced superoxide production and neurotoxicity in cultured rat hippocampal neurons: role of mitochondria. Eur J Neurosci 1998;10:1903-10.
16. Dugan LL, Gabrielesen JK, Yu SP, Lin T-S, Choi DW. Buckminsterfullerenol free radical scavengers reduce ex-cytotoxic and apoptotic death of cultured cortical neurons. Neurobiol Dis. 1996;3: 129-35, 305-10.
17. Budd SL, Nicholls DG. Mitochondria, calcium regulation, and acute glutamate excitotoxicity in cultured cerebellar granule cells. J Neurochem 1996;67:2282-91.
18. Monyer H, Hartley DM, Choi DW. 21-Aminosteroids attenuate excitotoxic neuronal injury in cortical cell cultures. Neuron 1990;5: 121-6.
19. Dugan LL, Turetsky DM, Du C, Lobner D, Wheeler M, Almli CR, et al. Carboxyfullerenes as neuroprotective agents. Proc Natl Acad Sci U S A 1997;94:9434-9.
20. Tauskela JS, Brunette E, O'Reilly N, Mealing G, Comas T, Gendron TF, et al. An alternative Ca^{2+}-dependent mechanism of neuroprotection by the metalloporphyrin class of superoxide dismutase mimetics. FASEB J 2005;19:1734-6.
21. Rosen GM, Britigan BE, Halpern HJ, Pou S. Free radicals, biology and detection by spin trapping. New York: Oxford University Press; 1999.
22. Utsumi H, Yamada K, Ichikawa K, Sakai K, Kinoshita Y, Matsumoto S, et al. Simultaneous molecular imaging of redox reactions monitored by Overhauser-enhanced MRI with ^{14}N- and ^{15}N-labeled nitroxyl radicals. Proc Natl Acad Sci U S A 2006;103:1463-8.
23. Sola M, Mestres J, Duran M. Molecular size and pyramidalization: two keys for understanding the reactivity of fullerenes. J Phys Chem 1995; 99:10752-8.
24. Haddon RC, Palmer RE, Kroto HW, Sermon PA. The fullerenes: powerful carbon-based electron acceptors. Philos Trans Phys Sci Eng 1993;343:53-62.
25. Diener MD, Alford JM. Isolation and properties of small-bandgap fullerenes. Nature 1998;393:668-71.
26. Ali SS, Hardt JI, Quick KL, Kim-Han JS, Erlanger BF, Huang TT, et al. A biologically effective fullerene (C60) derivative with superoxide dismutase mimetic properties. Free Radic Biol Med 2004;37:1191-202.
27. Ali SS, Xiong C, Lucero J, Behrens MM, Dugan LL, Quick KL. Gender differences in free radical homeostasis during aging: shorter-lived female C57BL6 mice have increased oxidative stress. Aging Cell 2006; 5:565-74.
28. Quick KL, Ali SS, Arch R, Xiong C, Wozniak D, Dugan LL. A carboxyfullerene SOD mimetic improves cognition and extends the lifespan of mice. Neurobiol Aging 2008;29:117-28.
29. Behrens MM, Ali SS, Dao DN, Lucero J, Shekhtman G, Quick KL, et al. Ketamine-induced loss of phenotype of fast-spiking interneurons is mediated by NADPH-oxidase. Science 2007;318:1645-7.
30. Koh JY, Choi DW. Quantitative determination of glutamate mediated cortical neuronal injury in cell culture by lactate dehydrogenase efflux assay. J Neurosci Methods 1987;20:83-90.
31. Furukawa H, Singh SK, Mancusso R, Gouaux E. Subunit arrangement and function in NMDA receptors. Nature 2005;438:185-92.
32. Furukawa H, Gouaux E. Mechanisms of activation, inhibition and specificity: crystal structures of the NMDA receptor NR1 ligand-binding core. EMBO J 2003;22:2873-85.
33. Wang X, Quinn PJ. The location and function of vitamin E in membranes. Mol Membr Biol 2000;17:143-56.
34. Quick KL, Hardt JI, Dugan LL. Rapid microplate assay for superoxide scavenging efficiency. J Neurosci Methods 2000;97:139-44.
35. McCord JM, Fridovich I. Superoxide dismutase. an enzymic function for erythrocuprein (hemocuprein). J Biol Chem 1969;244:6049-55.
36. Gotoh N, Niki E. Rates of interactions of superoxide with vitamin E, vitamin C and related compounds as measured by chemiluminescence. Biochim Biophys Acta 1992;1115:201-7.
37. Chen PE, Wyllie DJ. Pharmacological insights obtained from structure-function studies of ionotropic glutamate receptors. Br J Pharmacol 2006;147:839-53.
38. Dugan LL, Lovett E, Cuddihy S, Almli CR, Lin T-S, Choi DW. Carboxyfullerenes as neuroprotective antioxidants. In: Kreiglstein J, editor. Pharmacology of Cerebral Ischemia. New York: Academic Press; 1998. pp. 257-66.
39. Choi DW. Glutamate neurotoxicity and diseases of the nervous system. Neuron 1988;1:623-34.
40. Choi DW, Rothman SM. The role of glutamate neurotoxicity in hypoxic-ischemic neuronal death. Annu Rev Neurosci 1990;13:171-82.
41. Gardoni F, Di Luca M. New targets for pharmacological intervention in the glutamatergic synapse. Eur J Pharmacol 2006;545:2-10.
42. Foley S, Crowley C, Smaihi M, Bonfils C, Erlanger BF, Seta P, et al. Cellular localization of a water-soluble fullerene derivative. Biochem Biophys Res Commun 2002;294:116-9.
43. Lotharius J, Dugan LL, O'Malley KL. Distinct mechanisms underlie neurotoxin-mediated cell death in cultured dopaminergic neurons. J Neurosci 1999;19:1284-93.